On the presence of odd transverse convective rolls in narrow-gap horizontal annuli

Mark P. Dyko
Department of Mechanical Engineering, The Ohio State University, Columbus, Ohio 43210

Kambiz Vafai[a)]
Department of Mechanical Engineering, University of California, Riverside, California 92521

(Received 11 April 2001; accepted 29 November 2001)

A numerical study of three-dimensional supercritical states of natural convection in a narrow-gap horizontal cylindrical annulus is presented. For the first time, an odd number of counter-rotating transverse rolls is shown to occur in a narrow-gap annulus. Flow and temperature fields associated with the odd roll state are compared to those of transverse roll states exhibiting even numbers of rolls, and factors influencing the occurrence and number of odd rolls are investigated. © *2002 American Institute of Physics.* [DOI: 10.1063/1.1445423]

Natural convection in the annular space between concentric horizontal cylinders has been widely studied owing to its many technological applications. In most of the prior work, two-dimensional flow in a long annulus was investigated. Relatively few studies of three-dimensional flow, which occurs due to the presence of the end walls or the onset of thermal instabilities at higher Rayleigh numbers, are available in the literature. Previous investigations of three-dimensional natural convection in large- and moderate-gap annuli were directed toward classification of different convective regimes,[1–3] the effects of annulus inclination,[4] flow patterns in a short annulus,[5] temporal development of the flow and temperature fields,[6] turbulent flow,[7] and high Rayleigh number laminar flow.[8]

To the authors' knowledge, only Dyko and Vafai[9] have investigated three-dimensional natural convection in a narrow-gap annulus with end walls. Their results show the existence of two different supercritical states exhibiting even numbers of counter-rotating transverse rolls (axes of the rolls oriented in the angular direction) in the upper portion of the annulus, and two additional supercritical states having counter-rotating longitudinal rolls (axes parallel to the common axis of the inner and outer cylinders) in the highest part of the annulus in combination with transverse rolls located between the longitudinal rolls and primary flow. The presence of these four states is related to the onset of thermal instabilities in the horizontal layer formed locally by the upper part of the annulus.

In the present work, a fifth supercritical state characterized by odd numbers of transverse rolls in the upper portion of the annulus is discovered and investigated for the first time. The governing equations are formulated in terms of vorticity and vector potential and solved using a three-dimensional ADI method and the extrapolated Jacobi scheme. Simulations are performed at subcritical ($\mathrm{Ra} < \mathrm{Ra}_c$, where Ra_c is the critical Rayleigh number above which thermal instabilities set in) and supercritical ($\mathrm{Ra} > \mathrm{Ra}_c$) Rayleigh numbers to study the development and occurrence of different transverse roll supercritical states. Flow and temperature fields for the odd transverse roll state are compared to those for even transverse roll states, and the effects of varying annulus gap aspect ratio A on the odd roll state are examined.

The fluid layer is confined by inner and outer horizontal coaxial cylinders of length l having radii r_i and r_o, respectively, and two end walls that are oriented normal to the axis of the cylinders (Fig. 1). The temperature of the inner cylinder T_i is greater than that of the outer cylinder T_o, and the end walls are adiabatic. The nondimensional annulus length is defined by $L = l/r_i$. The annulus geometry is characterized by the gap aspect ratio $A = l/(r_o - r_i)$ and outer to inner cylinder radius ratio $R = r_o/r_i$. The computational domain is chosen to extend over the full radial ($1 \leqslant r \leqslant R$), angular ($-\pi \leqslant \phi \leqslant \pi$), and axial ($0 \leqslant z \leqslant L$) extent of the annulus.

The three-dimensional, transient, laminar, buoyancy-driven flow of an incompressible fluid is governed by the equations of conservation of mass, momentum, and energy. The momentum equation is simplified using the Boussinesq approximation. The pressure term is eliminated by taking the curl of the momentum equation, yielding the equation for transport of vorticity Ω. The vector potential Ψ is introduced for satisfying the conservation of mass and calculation of the velocity $\mathbf{V}$. From the equations defining vorticity and vector potential, a Poisson equation relating these two variables is obtained. The vorticity transport, Poisson, vector potential, and energy equations are solved for the ten unknowns Ω_r, Ω_ϕ, Ω_z, Ψ_r, Ψ_ϕ, Ψ_z, V_r, V_ϕ, V_z, and Θ.

Nondimensionalization of the conservation equations is accomplished using r_i for length, α/r_i for velocity, r_i^2/α for time, and $\rho\alpha^2/r_i^2$ for pressure, with α and ρ denoting the thermal diffusivity and density, respectively. The dimensionless temperature is defined by $\Theta = (T - T_o)/\Delta T$, where $\Delta T = T_i - T_o$. The dimensionless parameters Rayleigh number and Prandtl number are defined as $\mathrm{Ra}_r = g\beta r_i^3 \Delta T/\upsilon\alpha$ and $\mathrm{Pr} = \upsilon/\alpha$, respectively, where g is the acceleration due to

[a)]Author to whom correspondence should be addressed. Telephone: (909) 787-2135; Fax: (909) 787-2899. Electronic mail: vafai@engr.ucr.edu

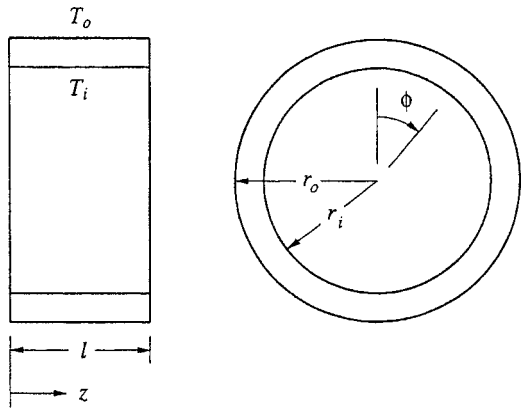

FIG. 1. Schematic figure of the horizontal annulus with end walls.

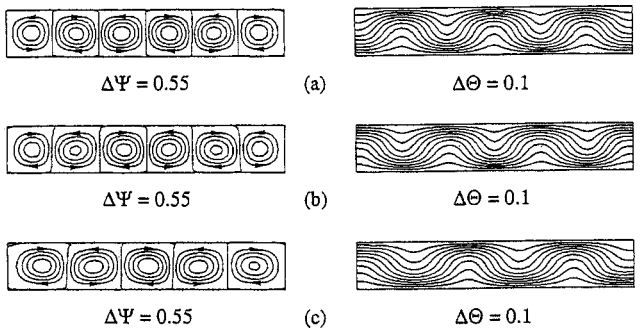

FIG. 2. Streamlines on the left and isotherms on the right at the upper vertical angular plane for $R=1.1$, $A=6$, $\mathrm{Ra}=2500$, $\mathrm{Pr}=0.7$: (a) first type of transverse roll pattern; (b) second type of transverse roll pattern; (c) third type of transverse roll pattern.

gravity, β is the coefficient of thermal expansion, and v the kinematic viscosity. The Rayleigh number $\mathrm{Ra}=g\beta(r_o-r_i)^3\Delta T/v\alpha$ is employed hereafter for convenience in comparing the results to those of previous studies.

Details of the numerical scheme, and a summary of comparisons of results to those of previous experimental and numerical investigations for verification of the accuracy of this scheme can be found in Dyko and Vafai.[9] In order to ensure the results are not dependent on grid size or time step size, the systematic mesh and time step refinement procedures they describe were employed in the present study.

All of the numerical simulations were performed over the full radial, angular, and axial extent of the annulus. The results of these simulations demonstrated that, due to flow symmetry, the normal velocity and the normal gradients of the tangential velocity components are zero at the vertical angular plane. Accordingly, the ϕ-component of vector potential corresponds to the two-dimensional stream function at this plane. The results are presented as streamlines and isotherms at the upper vertical angular plane ($\phi=0$) since these provide a representative cross-section of the flow patterns and temperature fields associated with the transverse rolls.

Simulations were conducted for an annulus filled with air ($\mathrm{Pr}=0.7$) having a radius ratio of $R=1.1$ and gap aspect ratio of $A=6$. The Rayleigh number was successively increased from subcritical to supercritical values to illustrate the development of the first type of supercritical transverse roll pattern, and gain insight into conditions leading to the occurrence of additional supercritical states. A comparison of supercritical states exhibiting only transverse rolls in the upper part of the annulus is made at a Rayleigh number of $\mathrm{Ra}=2500$. Results for gap aspect ratios in the range $4\leqslant A\leqslant 8$ are presented in the upcoming figures to illustrate the effects of varying annulus length on the odd transverse roll state.

At Rayleigh numbers less than the critical value for thermal instability of $\mathrm{Ra}_c=1740$ determined by Dyko and Vafai,[9] the flow in the annulus appears as two crescent shaped recirculation patterns centered near $\phi=\pm\pi/2$ when viewed in any axial plane. These patterns are symmetric to one another about the vertical angular plane. In the upper portion of the annulus, a weak transverse roll is present at each end wall that rotates clockwise and counterclockwise on the right- and left-hand sides of the annulus, respectively. These end rolls are driven by the main flow and form due to the viscous shear imposed by the end walls.

As the Rayleigh number is increased above Ra_c, two additional pairs of counter-rotating transverse rolls form in the upper part of the annulus between the end rolls due to thermal instability. The shear force that the pre-existing end rolls exert on the fluid in the inner region determines the directions of rotation of these inner rolls. At Rayleigh numbers immediately above Ra_c the inner rolls are weaker than the end rolls, but as the Rayleigh number is increased the strength of the inner rolls increases faster than that of the end rolls and becomes slightly greater. Due to the viscous shearing effect of the end walls, the end rolls remain weaker than the inner rolls as the Rayleigh number is elevated further.

The streamlines and isotherms in the upper vertical angular plane associated with the first type of supercritical transverse roll pattern described above are plotted on the left- and right-hand sides, respectively, of Fig. 2(a) for $R=1.1$, $A=6$, and $\mathrm{Ra}=2500$. The greater strength of the inner rolls as compared to the end rolls is evident from the closer spacing of streamlines within the inner rolls. The alternating rise and fall of the isotherms along the length of the annulus reflects the opposing directions of rotation of the rolls. The isotherms are spaced more closely to the inner and outer cylinders where the fluid cooled by the outer cylinder impinges on the inner cylinder and the fluid heated by the inner cylinder impinges on the outer cylinder, respectively.

In the absence of perturbations in the flow and temperature fields, the first type of transverse roll pattern arises when starting from a quiescent and isothermal state and increasing the Rayleigh number to a value above Ra_c. This occurs because the end rolls develop prior to formation of the supercritical rolls, thereby inducing formation of the same supercritical transverse rolls described so far. Even under carefully controlled conditions, however, small disturbances may occur that trigger instabilities resulting in formation of the supercritical rolls before development of these end rolls. In this situation, the orientations and directions of roll rotation are no longer predetermined and additional types of supercritical roll patterns can develop.

To simulate such a process using a numerical scheme in which round-off errors are negligible, disturbances must be

intentionally introduced. This was accomplished by specifying the following perturbed temperature field at $t=0$:

$$\Theta = 1 - (\ln r/\ln R) + C_A \sin(\pi \ln r/\ln R)(-\cos(C_B \pi z + \eta)), \tag{1}$$

where C_A is an amplification coefficient, C_B is the wave number, and η is the phase shift of the temperature perturbation. The initial condition prescribed by Eq. (1) physically represents the reversal of thermal gradients associated with inception of thermal instabilities in the annulus. Since Eq. (1) is periodic in the z direction, it triggers the formation of transverse rolls.

To investigate different transverse roll supercritical states, simulations were conducted in which C_B and η in Eq. (1) were independently varied. Using a value of C_B based on the first type of transverse roll pattern, it was found that varying η over the range $0 \leqslant \eta \leqslant 2\pi$ resulted in either the first type of steady transverse roll pattern or a second steady transverse roll pattern exhibiting the same number of rolls as the first type but with opposite directions of rotation. These results are consistent with the findings of Dyko and Vafai.[9] The streamlines and isotherms in the upper vertical angular plane for the second type of supercritical transverse roll pattern are plotted on the left- and right-hand sides, respectively, of Fig. 2(b) for $R=1.1$, $A=6$, and $\mathrm{Ra}=2500$. By comparing Fig. 2(b) with Fig. 2(a), it is seen that each roll rotates in a direction opposite that of the corresponding roll in the first type of transverse roll pattern. Accordingly, the alternating elevation and depression of isotherms along the length of the annulus for the second type of transverse roll pattern is opposite that of the first type.

From the simulations in which C_B was independently varied (affecting the number of initial rolls), a third type of transverse roll pattern exhibiting an odd number of sustained rolls at steady state was discovered. For a gap aspect ratio of $A=6$ with $R=1.1$ and $\mathrm{Ra}=2500$, it was found that the presence of five initial transverse rolls resulted in five sustained rolls at steady state. Likewise, six initial rolls carried over to six sustained rolls. For other than five or six initial transverse rolls, the initial number of rolls was not sustained. Instead, after a sufficient period of time elapsed the flow transitioned to the first type of transverse roll pattern, which has six rolls. The streamlines and isotherms in the upper vertical angular plane associated with the third type of transverse roll pattern are presented on the left- and right-hand sides, respectively, of Fig. 2(c) for $R=1.1$, $A=6$, and $\mathrm{Ra}=2500$. It is seen that the two end rolls rotate in the same direction as one another, as is always the case for an odd number of counter-rotating rolls. With an even number of counter-rotating rolls, the end rolls rotate in opposite directions as seen in Figs. 2(a) and 2(b).

Owing to differences in the number of rolls and directions of roll rotation, the impingement regions on the inner and outer cylinders are somewhat different for each of the transverse roll patterns. These regions are indicated by the closer spacing of isotherms next to the cylinder walls seen in Figs. 2(a), 2(b), and 2(c) for the first, second, and third types of transverse roll patterns, respectively. There are four inner cylinder and three outer cylinder impingement regions for the first transverse roll pattern, compared to three inner cylinder and four outer cylinder impingement regions for the second transverse roll pattern. With the third transverse roll pattern, there are three inner cylinder and three outer cylinder impingement regions for a total of six impingement regions, which is one fewer than for the first and second patterns.

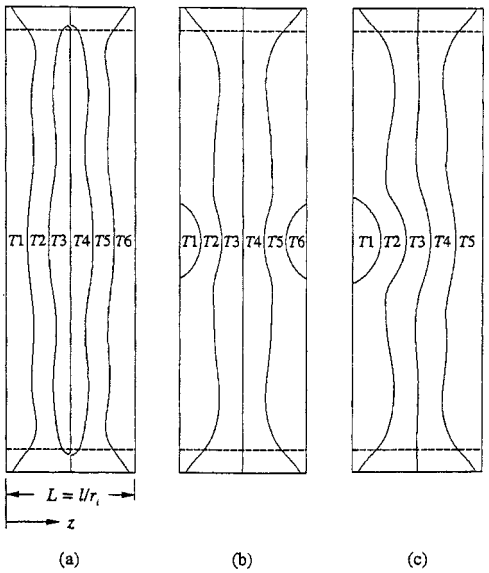

FIG. 3. Boundaries of the steady convective rolls in the upper portion of the annulus (as viewed from above the annulus looking downward) for $R=1.1$, $A=6$, $\mathrm{Ra}=2500$, $\mathrm{Pr}=0.7$: (a) first type of transverse roll pattern; (b) second type of transverse roll pattern; (c) third type of transverse roll pattern.

Overall representations of the different transverse roll patterns are provided in Fig. 3 for $R=1.1$, $A=6$, and $\mathrm{Ra}=2500$. Schematic diagrams of the convective roll boundaries in the upper region of the annulus are plotted in Figs. 3(a), 3(b), and 3(c) for the first, second, and third types of transverse roll patterns, respectively. The view is from above the annulus looking downward. It is seen in Figs. 3(a) and 3(b) that the first and second types of transverse roll patterns each exhibit six rolls ($T1-T6$) in the upper portion of the annulus. The third type of transverse roll pattern exhibits five rolls ($T1-T5$) as seen in Fig. 3(c). By comparing Fig. 3(c) with Fig. 3(a), it is seen that the boundaries of the end roll ($T5$) on the right-hand side of the annulus for the third type of transverse roll pattern are similar to the end roll ($T1$ and $T6$) boundaries for the first type of transverse roll pattern. The direction of fluid movement adjacent to the end wall is the same for each of these three end rolls, with the flow proceeding downward along the wall [see Figs. 2(a) and 2(c)]. Similarly, from Figs. 3(c) and 3(b) it is seen that the boundaries of the end roll on the left-hand side of the annulus ($T1$) for the third type of transverse roll pattern are similar to the end roll ($T1$ and $T6$) boundaries for the second type of transverse roll pattern. For these three end rolls, which are of more limited angular extent than the other end rolls, the flow moves upward next to the end walls [see Figs. 2(b) and 2(c)].

To investigate the influence of gap aspect ratio A on the third type of transverse roll pattern, simulations were con-

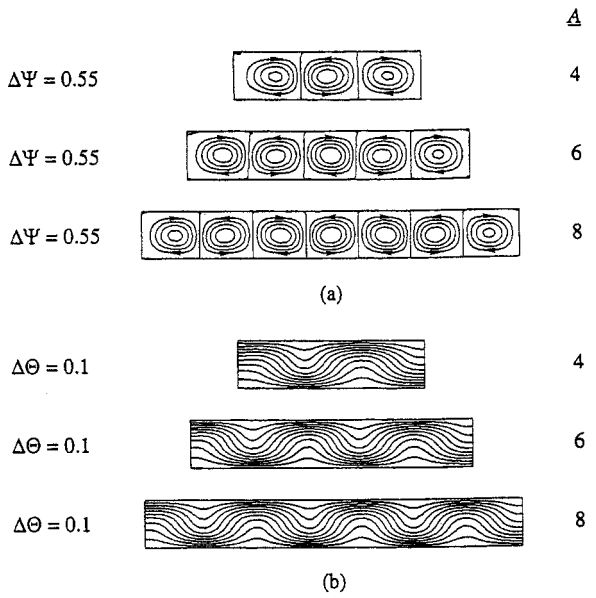

FIG. 4. Effect of annulus length on convection at the upper vertical angular plane for the third type of transverse roll pattern for $R=1.1$, $\mathrm{Ra}=2500$, $\mathrm{Pr}=0.7$: (a) streamlines; (b) isotherms.

ducted for $A=4$, 5, 6, 7, and 8 with $R=1.1$ and $\mathrm{Ra}=2500$, using values of C_B corresponding to odd numbers of initial rolls. For the even-integer gap aspect ratios $A=4$, 6, and 8, it was found that an odd number of rolls equal to $n=A-1$ was sustained at steady state. The streamlines and isotherms in the upper vertical angular plane associated with these odd roll patterns are presented in Figs. 4(a) and 4(b), respectively, for $R=1.1$ and $\mathrm{Ra}=2500$. For the odd-integer gap aspect ratios $A=5$ and 7, odd numbers of transverse rolls were not sustained at steady state. Instead, the initial odd rolls transitioned to four and six steady transverse rolls for $A=5$ and 7, respectively. These results indicate that for the odd-integer values of A within the range of $4\leqslant A\leqslant 8$ that was studied, an even number of rolls is preferred.

Simulations were also performed for non-integer values of A with $R=1.1$ and $\mathrm{Ra}=2500$ to obtain further insight into the effect of A on occurrence of the third type of transverse roll pattern. From these simulations, it was found that an odd number of rolls is preferred for certain gap aspect ratios that would require either relatively large or small roll sizes (compared to typical roll sizes) for an even number of rolls to fit in the annulus. One such case is $A=5.8$, which would need either four very large rolls or six small rolls. For this case, five rolls were sustained in the annulus at steady state regardless of the initial conditions. When starting from quiescent and isothermal initial conditions or successively increasing the Rayleigh number from subcritical to supercritical values, six rolls would initially form, but these transitioned to five steady rolls after a sufficient period of time. It is noted that a similar preference for odd rolls in rectangular boxes with gap aspect ratios that would require either relatively large or small roll sizes for an even number of rolls to fit in the box was observed in the experiments of Stork and Muller.[10]

In addition to the cases analyzed for $R=1.1$ with $\mathrm{Ra}=2500$, simulations were carried out for $R=1.05$ and 1.15 with $A=6$ and $\mathrm{Ra}=2500$, and for Rayleigh numbers in the range $1700\leqslant \mathrm{Ra}\leqslant 2500$ with $R=1.1$ and $A=6$ to study the effects of annulus radius ratio and Rayleigh number, respectively. From these studies, it was determined that the third type of transverse roll pattern arises in annuli with a radius ratio R less than a critical value R_3, where $1.1<R_3<1.15$. The Rayleigh number above which this pattern is sustained was found to be approximately $\mathrm{Ra}=2480$ for $R=1.1$ and $A=6$, as compared to $\mathrm{Ra}_c=1740$ and $\mathrm{Ra}=1950$ for the first and second types of transverse roll patterns, respectively.

In conclusion, our studies have shown that a supercritical state exhibiting an odd number of transverse rolls in the upper portion of the annulus can occur in a narrow-gap annulus with end walls. This state is distinguished from other transverse roll states by the number of rolls and the presence of end rolls that rotate in the same direction as one another. The occurrence and number of odd rolls were shown to be dependent on the gap aspect ratio A. Odd numbers of rolls were sustained at steady state in an annulus of $R=1.1$ for gap aspect ratios within the range of $4\leqslant A\leqslant 8$ that was studied, except for two sub-ranges of A encompassing the odd-integers $A=5$ and 7, respectively. For the even-integers $A=4$, 6, and 8, the number of sustained odd rolls was $n=A-1$. It was found that the odd roll state can arise when the inception of instability occurs prior to development of the end rolls, and/or for certain gap aspect ratios that would require either very large or small roll sizes for an even number of rolls to fit in the annulus.

ACKNOWLEDGMENT

We gratefully acknowledge a grant from the Ohio Supercomputer Center.

[1] U. Grigull and W. Hauf, "Natural convection in horizontal cylindrical annuli," Proceedings of the 3rd International Heat Transfer Conference **2**, 182 (1966).
[2] R. E. Powe, C. T. Carley, and E. H. Bishop, "Free convective flow patterns in cylindrical annuli," Trans. ASME, Ser. C: J. Heat Transfer **91**, 310 (1969).
[3] Y. F. Rao, Y. Miki, K. Fukuda, Y. Takata, and S. Hasegawa, "Flow patterns of natural convection in horizontal cylindrical annuli," Int. J. Heat Mass Transf. **28**, 705 (1985).
[4] Y. Takata, K. Iwashige, K. Fukuda, and S. Hasegawa, "Three-dimensional natural convection in an inclined cylindrical annulus," Int. J. Heat Mass Transf. **27**, 747 (1984).
[5] T. Fusegi and B. Farouk, "A three-dimensional study of natural convection in the annulus between horizontal concentric cylinders," Proceedings ofthe 8th International Heat Transfer Conference **4**, 1575 (1986).
[6] K. Vafai and J. Ettefagh, "An investigation of transient three-dimensional buoyancy driven flow and heat transfer in a closed horizontal annulus," Int. J. Heat Mass Transf. **34**, 2555 (1991).
[7] C. P. Desai and K. Vafai, "An investigation and comparative analysis of two- and three-dimensional turbulent natural convection in a horizontal annulus," Int. J. Heat Mass Transf. **37**, 2475 (1994).
[8] M. P. Dyko, K. Vafai, and A. K. Mojtabi, "A numerical and experimental investigation of stability of natural convective flows within a horizontal annulus," J. Fluid Mech. **381**, 27 (1999).
[9] M. P. Dyko and K. Vafai, "Three-dimensional natural convective states in a narrow-gap horizontal annulus," J. Fluid Mech. **445**, 1 (2001).
[10] K. Stork and U. Muller, "Convection in boxes: experiments," J. Fluid Mech. **54**, 599 (1972).